ARTICLE
Journal of Cellular Biochemistry 109:576–584 (2010)

Journal of Cellular Biochemistry

S100A6 (Calcyclin) Deficiency Induces Senescence-Like Changes in Cell Cycle, Morphology and Functional Characteristics of Mouse NIH 3T3 Fibroblasts

Łukasz P. Słomnicki and Wiesława Leśniak*

Department of Molecular and Cellular Neurobiology, Nencki Institute of Experimental Biology, 3 Pasteur St, 02-093 Warsaw, Poland

ABSTRACT

S100A6 (calcyclin) is a calcium binding protein with two EF-hand structures expressed mostly in fibroblasts and epithelial cells. We have established a NIH 3T3 fibroblast cell line stably transfected with siRNA against S100A6 to examine the effect of S100A6 deficiency on non-transformed cell physiology. We found that NIH 3T3 fibroblasts with decreased level of S100A6 manifested altered cell morphology and proliferated at a much slower pace than the control cells. Cell cycle analysis showed that a large population of these cells lost the ability to respond to serum and persisted in the G0/G1 phase. Furthermore, fibroblasts with diminished S100A6 level exhibited morphological changes and biochemical features of cellular senescence as revealed by β-galactosidase and gelatinase assays. Also, S100A6 deficiency induced changes in the actin cytoskeleton and had a profound impact on cell adhesion and migration. Thus, we have shown that the S100A6 protein is involved in multiple aspects of fibroblast physiology and that its presence ensures normal fibroblast proliferation and function. J. Cell. Biochem. 109: 576–584, 2010.

KEY WORDS: S100A6; CALCYCLIN; SENESCENCE; PROLIFERATION; NIH 3T3 FIBROBLASTS; CELL MOTILITY

S100A6 (calcyclin) is a representative of the S100 family of small calcium-binding proteins with two EF-hand structures [Santamaria-Kisiel et al., 2006]. Its gene expression is cell specific and may depend on DNA methylation [Lesniak et al., 2007]. S100A6 is typical for fibroblasts and epithelial cells [Kuznicki et al., 1992] and is often increased in cancers of epithelial origin [Weterman et al., 1992; Komatsu et al., 2000]. In vitro, an increase in S100A6 mRNA and/or protein level can be induced by multiple agents [Kucharczak et al., 2001; Courtois-Coutry et al., 2002]. Moreover, recent studies have shown upregulation of S100A6 in cells exposed to various stressful conditions such as oxidative stress or hypoxia [Lesniak et al., 2005; Cervera et al., 2008]. Ever since the identification of its mRNA among those upregulated when quiescent cells were induced to proliferate [Hirschhorn et al., 1984] S100A6 was suggested to take part in the regulation of cell cycle. Nonetheless, the biological role of S100A6 remains unresolved and may be inferred only indirectly from the ever-growing number of reports on its interactions with other proteins [Zeng et al., 1993; Filipek et al., 1995; Golitsina et al., 1996; Filipek and Kuźnicki, 1998; Nowotny et al., 2003]. A convenient and validated model to study the function of a protein is to look for differences between wild type cells, cells overexpressing the protein and/or those devoid of it. Several attempts of that sort have been made and rendered interesting information on the role of S100A6. It was shown that S100A6 overexpression leads to higher cell proliferation rate and sensitizes cells to apoptosis [Hwang et al., 2004; Joo et al., 2008]. On the other hand transient transfection with S100A6 antisense or siRNA inhibited cell proliferation and invasive potential and changed cell morphology [Breen and Tang, 2003; Hwang et al., 2004; Ohuchida et al., 2007]. Most of these studies were however performed on transiently transfected cells allowing only for observation of short-term effects and/or examined a relatively narrow spectrum of changes. We have established a NIH 3T3 fibroblast cell line stably transfected with siRNA against S100A6 to examine the effect of S100A6 deficiency on non-transformed cell physiology in a longer time scale. We report that the presence of S100A6 seems to be critical for fibroblast proliferation since its deficiency, as evidenced by cell cycle analysis, prolongs the G0/G1 phase and leads to cell cycle withdrawal of a significant number of cells. Such cells acquire many features of the senescent phenotype including high β-galactosidase activity and an altered morphology accompanied by changes in adhesive and motile properties.

*Correspondence to: Wiesława Leśniak, Department of Molecular and Cellular Neurobiology, Nencki Institute of Experimental Biology, 3 Pasteur St., 02-093 Warsaw, Poland. E-mail: w.lesniak@nencki.gov.pl
Received 5 May 2009; Accepted 27 October 2009 • DOI 10.1002/jcb.22434 • © 2009 Wiley-Liss, Inc.
Published online 9 December 2009 in Wiley InterScience (www.interscience.wiley.com).

MATERIALS AND METHODS

CELL CULTURE AND ESTABLISHMENT OF STABLY TRANSFECTED MOUSE NIH 3T3 FIBROBLASTS

NIH 3T3 mouse fibroblasts were cultured in Dulbecco's Modified Eagle's Medium (DMEM) (Sigma) supplemented with 10% fetal bovine serum (FBS) (Gibco), 100 U/ml penicillin, 100 μg/ml streptomycin (Sigma) in an incubator at 37°C and 5% CO_2. The cells were transfected using Lipofectamine2000 with the pSilencer 2.1-U6 hygro vector (Ambion) encoding short hairpin RNA comprising either a 19 bp long S100A6 siRNA sequence (5′-GCCUUGGCUUUGAUCUACA-3′) or a control siRNA sequence with no significant homology to mammalian genomes, present in the manufacturer's set. The vector used for transfections was either intact or linearized with SalI restriction enzyme. Further details on vectors and cloning are described by Slomnicki et al. [2009]. Hygromycin (400 μg/ml) was added to the medium 48 h after transfection and cells were maintained in these conditions for 14 days with dying cells being regularly washed out. Remaining cells (from four independent transfections with vector containing S100A6 siRNA and from one transfection with control plasmid) were propagated in the presence of 200 μg/ml hygromycin, examined for S100A6 expression by Western blot (Fig. 1) and portions were frozen.

ANTIBODIES

The following antibodies were used: polyclonal rabbit anti-S100A6 described in Filipek et al. [1993], mouse monoclonal anti-GAPDH (Chemicon International), mouse monoclonal anti-vinculin (Sigma), anti-rabbit IgG FITC-conjugated (Sigma), anti-rabbit IgG peroxidase conjugated (MP Biomedicals), anti-mouse IgG peroxidase-conjugated (Jackson Immunoresearch) and anti-mouse IgG Alexa Fluor 568-conjugated (Invitrogen).

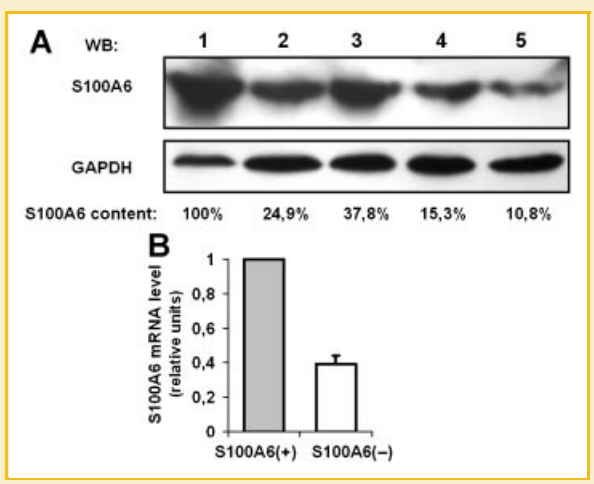

Fig. 1. The level of S100A6 in stably transfected S100A6(+) and S100A6(−) NIH 3T3 fibroblasts. A: S100A6 protein level in cells transfected with a control plasmid (1) or plasmid coding siRNA for S100A6 in a circular (2, 3) or linearized form (4, 5). Electrophoresis was performed using 350 μg of total cell extract and Western blot was developed with anti-S100A6 antibody (upper panel) and anti-GAPDH antibody (lower panel). B: S100A6 mRNA level in cells transfected with a control plasmid (S100A6(+), lane 1 in A) or plasmid coding siRNA for S100A6 (S100A6(−), lane 5 in A) examined by Real Time-PCR.

WESTERN BLOT ANALYSIS

Cells were washed with ice-cold PBS and lysed with 50 mM Tris–HCl, pH 7.5, 0.1% Triton X-100, 1 mM EDTA, 2 mM $CaCl_2$ with complete protease inhibitors, and homogenized by insulin-like syringe pipetting. Samples were centrifuged at 10,000*g* at 4°C for 10 min. The proteins in the supernatants were separated by 15% SDS-PAGE and transferred onto a nitrocellulose membrane. The blot was incubated with rabbit anti-S100A6 antibody diluted 250 times and developed with secondary peroxidase-conjugated anti-rabbit IgG antibody diluted 5,000 times. Results were relativized to the GAPDH immunodetection signal. The primary anti-GAPDH antibody was used at a 10,000× dilution and the secondary anti-mouse IgG antibody at 15 000× dilution.

RNA ISOLATION AND REAL TIME PCR ANALYSIS

NIH 3T3 fibroblast RNA was isolated with the RNeasy kit (Qiagen) and S100A6 cDNA was synthesized using the M-MLV reverse transcriptase (Sigma). S100A6 cDNA level was quantified by Real Time PCR using the SYBR-green master mix and the Applied Biosystems hardware and software (7500 Real Time PCR System). Results were relativized to the results obtained for GAPDH cDNA. The S100A6 primers were: 5′-TTCTCGTGGCCATCTTCCACAAGT-3′ and 5′-TGGTGAGCTCCTTCTGGATCAACT-3′ and these for GAPDH: 5′-CAGTGGCAAAGTGGAGATTG-3′ and 5′-AATTTGCCGTGAGTG-GAGTC-3′.

CELL SIZE AND PROLIFERATION

S100A6(−) and S100A6(+) NIH 3T3 fibroblasts were photographed under a phase contrast microscope (200× magnification). At least 40 single cells were outlined using the ImageJ software and their area was calculated. For the proliferation assay, cells were counted in the Neubauer chamber and plated onto six-well dishes at the density of 10^5 cells per well. After 68 and 110 h, cells were collected by trypsinization, counted and the population doubling (PD) factor was calculated.

FLOW CYTOMETRY ANALYSIS (FACS ANALYSIS)

S100A6(−) and S100A6(+) NIH 3T3 fibroblasts were synchronized by 48 h starvation and analyzed at 0, 16.5, and 19.5 h after addition of media containing 10% FBS. Cells were harvested, pelleted and resuspended in 70% ice-cold ethanol for 1 h. After centrifugation at 300*g* for 5 min, cells were resuspended in PBS containing 50 μg/ml propidium iodide (PI), 0.1% sodium citrate, 10 μg/ml RNase A and 0.1% Triton X-100, incubated for 30 min in the dark, and analyzed in FACSCalibur (Becton Dickinson). The percentage of cells in a particular cell cycle stage was calculated by the ModFit software (Becton Dickinson) employing a stable G2/G1 ratio of 1.82. In another experimental option, cells were washed in PBS and resuspended in intracellular staining buffer (PBS supplemented with 0.1% Triton X-100, 3% BSA and 0.02% sodium azide) for 0.5 h. Anti-S100A6 polyclonal antibody was then added for 1 h at room temperature. Cells were washed 3 times in the staining buffer and incubated with the anti-rabbit IgG FITC-conjugated antibody,

diluted 500 times, for 30 min in the dark. In the next step fibroblasts were stained with PI as described above and analyzed by two-color flow cytometry (FACSCalibur, Becton Dickinson).

β-GALACTOSIDASE ASSAY

After 48 h of culture S100A6(−) and S100A6(+) NIH 3T3 fibroblasts were washed twice with PBS and fixed with 2% formaldehyde, 0.2% glutaraldehyde, in PBS, for 15 min at room temperature. Then, cells were washed twice with PBS and incubated at 37°C in staining solution (sodium phosphate buffer, pH 6.0, 150 mM NaCl, 2 mM $MgCl_2$, 5 mM potassium ferrocyanure, 5 mM potassium ferricyanure, 1 mg/ml 5-bromo-4-chloro-3-indolyl-D-galactoside) for 16 h. Cells were washed twice with PBS and the dark blue-dyed cells positive for β-galactosidase were counted [Dimri et al., 1995].

ZYMOGRAPHY ANALYSIS

Analysis of extracellular matrix metalloproteinases (gelatinases) activity was performed as described in Kossakowska et al. [1999]. Stably transfected NIH 3T3 fibroblasts were cultured at high density in medium containing 0.5% FBS for 2 days. Cell culture medium (15 μl) was collected, mixed with 5 μl of gel loading buffer (62.5 mM Tris–HCl, 7.5 pH, 2% SDS, 10% glycerol, 0.002% bromophenol blue) and applied onto 10% polyacrylamide gel co-polymerized with 2 mg/ml porcine gelatin (Sigma). After electrophoresis the gel was washed twice in 50 mM Tris–HCl, 7.5 pH, 2.5% Triton X-100 and again in 50 mM Tris–HCl, 7.5 pH. It was then incubated at 37°C for 24 h in the zymography buffer (50 mM Tris–HCl, 7.5 pH, 5 mM $CaCl_2$, 1 μM $ZnCl_2$, 0.02% sodium azide), stained in 0.2% Coomassie brilliant blue (prepared in 10% acetic acid, 10% isopropanol) and the gelatinolytic activity manifested by unstained proteolytic zones was quantified employing the Gene Tools software (SynGene).

IMMUNOCYTOCHEMISTRY

Stably transfected S100A6(−) and S100A6(+) NIH 3T3 fibroblasts were plated onto slides at a low density. After 24 h cells were fixed by 3% paraformaldehyde for 20 min, treated with 50 mM NH_4Cl and permeabilized with 0.1% Triton X-100 (all reagents were diluted in buffer containing: 60 mM PIPES, 25 mM HEPES, pH 9.6, 10 mM EGTA, 4 mM $MgCl_2$). After preincubation with 3% BSA in PBS for 2 h cells were stained and analyzed by confocal microscopy (Leica) at 630× magnification. Actin microfilaments were stained with 1 μg/ml phalloidin (phalloidin-tetramethylrhodamine B isothiocyanate, Sigma). Vinculin was stained by anti-vinculin antibody used at a 1:100 dilution and an anti-mouse Alexa Fluor 568-conjugated secondary antibody diluted 200 times. Nuclei were stained with DAPI (1.5 μg/μl) present in the Vectashield mounting medium (Vector Lab).

CELL ADHESION ASSAY

To measure adhesion of the S100A6(−) and S100A6(+) NIH 3T3 fibroblasts we employed the CytoSelect 48-Well Cell Adhesion Assay (Cell Biolabs). Cells were seeded at the density of 10^5 per well in a serum free media and the assay was performed according to manufacturer's instructions. Sample absorbance was measured at 620 nm using a 96-well plate and a Multiscan RC (ThermoLabsystems) multi-well spectrophotometer. Cell adhesion to fibronectin was additionally examined in wells coated with fibronectin (15 μg/ml in PBS) for 1 h at 37°C and then blocked by incubation in 2% heat-inactivated BSA in PBS for 1 h.

CELL MOBILITY ASSAYS

Artificial wound (scratch) assay—a scratch was made with a 0.2 ml pipette tip through a monolayer of S100A6(−) and S100A6(+) NIH 3T3 fibroblasts grown on 60 mm dish coated with 15 μg/ml fibronectin (Sigma). Cell debris was washed up and a new portion of medium was added. Images of five different areas along the artificial wound were made and the number of cells found in the central part of the scratch (corresponding to half of its original width) was counted after 36 h.

Random migration analysis—stably transfected NIH 3T3 fibroblasts were seeded on dishes coated with fibronectin as described above at a density of 5×10^4cells/well in a regular culture medium and after 24 h were placed in an environmental chamber (37°C, 5% CO_2) of a Leica DMI6000 microscope. Images were collected using a polarization contrast at 100× magnification at 5 min intervals over 150 min with a video camera (Leica). To track the migration path of individual cells, cells were manually traced for each frame using the ImageJ software. The migration paths were prepared as graphs using the Excel software (Microsoft).

RESULTS

PHENOTYPIC CHANGES IN S100A6(−) NIH 3T3 FIBROBLASTS

Mouse NIH 3T3 fibroblasts stably transfected with the pSilencer 2.1 plasmid encoding siRNA against S100A6 demonstrated diminished levels of the S100A6 protein (Fig. 1A). Cells with the lowest S100A6 content (10.8% of control, Fig. 1A, lane 5) were additionally examined for S100A6 mRNA level and found to contain less than 50% of the original amount of mRNA (Fig. 1B). These cells, designated as S100A6(−) cells/fibroblasts, and cells transfected with the control plasmid, designated as control or S100A6(+) cells, were used for all subsequent studies. The S100A6(−) fibroblasts revealed an altered phenotype manifested by a more flattened appearance and a bigger size; also their nuclei looked bigger and were better discernible in a phase contrast microscope. When quantified using the ImageJ software, the average size of a S100A6(−) cell ($219.91 \pm 10.4\ \mu m^2$) was 1.6 times bigger than the size of a control S100A6(+) cell ($135.79 \pm 4.7\ \mu m^2$). Furthermore, a lot of the S100A6(−) NIH 3T3 fibroblasts lost their typical spindle shape and became polygonal. Many of the features mentioned above were reminiscent of senescent cells; this notion was further reinforced by the observation that the control S100A6(+) NIH 3T3 fibroblasts became confluent faster in comparison with the S100A6(−) cells. This was due to a dramatically decreased proliferation rate of the latter cells as evaluated by the proliferation assay (Fig. 2). Accordingly, the population doubling (PD) time of the S100A6(−) NIH 3T3 fibroblasts appeared to be almost 3 times longer than the PD of the S100A6(+) cells (Fig. 2). All these observations suggested that

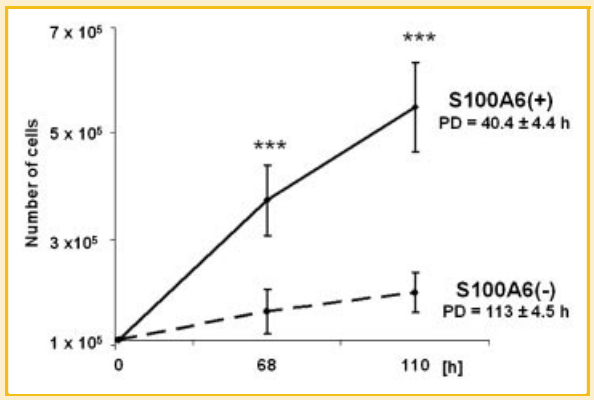

Fig. 2. Cell proliferation assay. Cells were counted in the Neubauer chamber before plating and after 68 and 110 h of culture. Statistical analysis was performed using Student's *t*-test. Results are mean ± SEM of three experiments, $^{***}P \leq 0.001$. The calculated population doubling time (PD) is given.

the presence of the S100A6 protein is vital not only for fibroblast morphology but, more importantly, for the proper regulation of fibroblast proliferation/quiescence. We decided to investigate in more detail the impact of the S100A6 protein on these processes by comparing various aspects of the S100A6 (−) and S100A6(+) NIH 3T3 fibroblast physiology.

COMPARISON OF THE CELL CYCLE IN S100A6(−) AND S100A6(+) NIH 3T3 FIBROBLASTS

Cells were synchronized by starvation and the progress of cell cycle was analyzed at different time intervals after serum stimulation. Initial experiments performed on wild type NIH 3T3 fibroblasts served to establish the time points, 16.5 and 19.5 h respectively, corresponding roughly to the peaks of the S and G2/M phases. We observed that 16.5 h after serum addition the S100A6(−) NIH 3T3 fibroblasts lagged behind the control ones and largely persisted in the G0/G1 phase. The amount of cells still in the G0/G1 phase was 6.5% higher than in the case of the S100A6(+) fibroblasts (Fig. 3A). Accordingly, after 19.5 h, when the majority of S100A6(+) cells have already reached the G2/M phase, the largest fraction of the S100A6(−) cells was still in the S phase. Although the differences in the amount of cells in the G0/G1 and S phases and the S and G2/M phases were statistically significant ($P < 0.01$) after 16.5 and 19.5 h, respectively, they did not correspond to the huge difference in S100A6 content between the S100A6(+) and S100A6(−) NIH 3T3 fibroblasts. It was also not clear if these differences were due to a prolonged G0/G1 phase, general cell cycle slow-down or a cell cycle withdrawal of a certain S100A6(−) cell population. Since siRNA could inhibit S100A6 expression to a different extent in individual cells we endeavored to perform the cell cycle analysis on cells with the lowest S100A6 content. For that we immunostained cells with anti-S100A6 antibody and performed a two-color flow cytometry

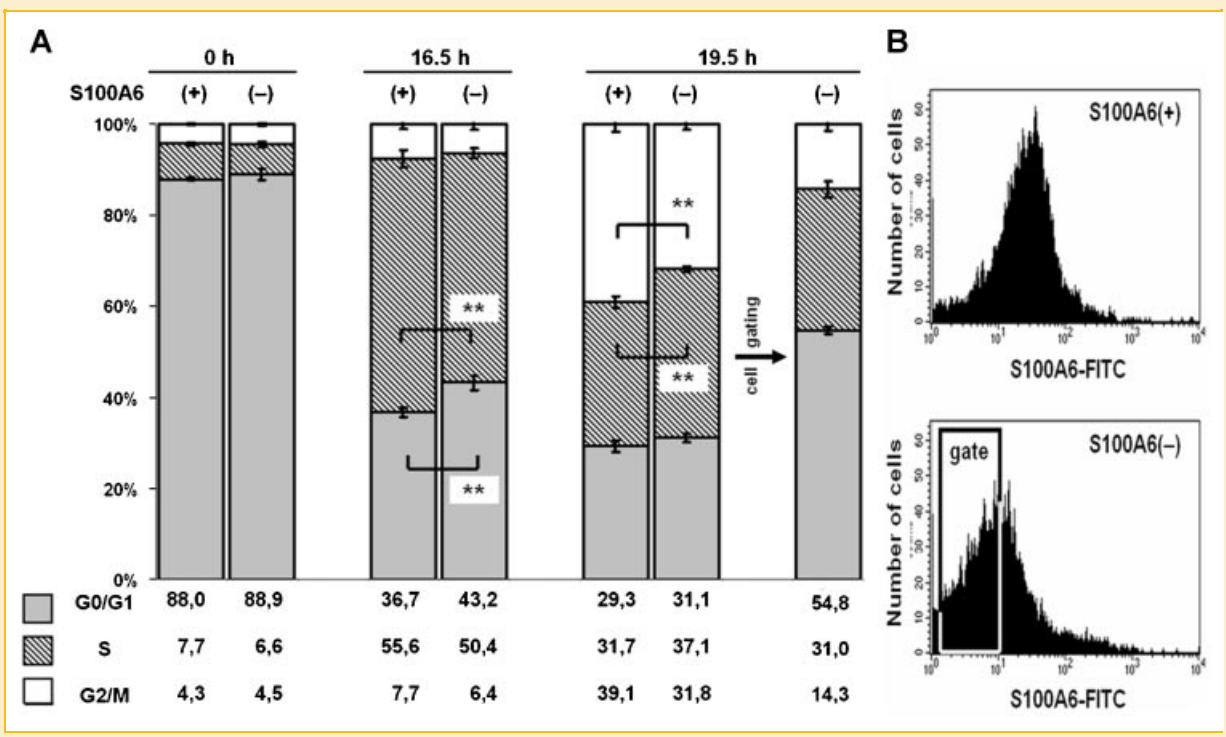

Fig. 3. Cell cycle analysis. A: Stably transfected NIH 3T3 cells were synchronized by 48 h starvation. Cell cycle analysis was performed at the end of starvation (0 h) and 16.5 and 19.5 h after FBS addition. The percentage of cells in the G0/G1 (gray), S (stripes) and G2/M (white) phases of cell cycle was calculated employing the ModFit software provided by Becton Dickinson. Statistical analysis was performed using Student's *t*-test. Results of three independent experiments are presented as a mean ± SEM; $^{**}P \leq 0.01$. B: S100A6(+) and S100A6(−) NIH 3T3 fibroblasts were stained with anti-S100A6 antibody followed by FITC-coupled secondary antibody and analyzed by two-color flow cytometry 19.5 h after the end of starvation. Cells with the lowest S100A6 protein content (RFU < 10) within the S100A6(−) cell population were gated and their cell cycle was analyzed separately (last bar in panel A). Representative histograms and the established gate are shown.

analysis. As expected (Fig. 3B), the S100A6(−) NIH 3T3 fibroblasts revealed a lower FITC staining intensity than control cells. The median value of the FITC signal was 21.15 ± 0.56 and 8.15 ± 0.2 RFU (relative fluorescence unit) for the S100A6(+) and S100A6(−) cells, respectively. Within the latter cell population we have arbitrarily assigned cells with the FITC signal strength lower than 10 RFU (indicated by frame in Fig. 3B) and analyzed their cell cycle separately. Differences in the cell cycle characteristics of these cells were evident even in the non-synchronized cell population: cells in the G0/G1-phase constituted 87.7% of the population, compared to 69.7% of control S100A6(+) cells while the respective values for the S phase were 9.1% and 17.5% (not shown). The contrast was further elevated when we analyzed synchronized cells. For instance, at the peak of the G2/M phase, 19.5 h after the end of starvation, in subpopulation with the lowest S100A6 content 54.8% of cells were in the G0/G1 phase and only 14.3% in the G2/M phase (Fig. 3A, last bar). These data show that the lack of S100A6 expression results in a massive cell retention in the G0/G1 phase possibly followed by cell cycle withdrawal and suggest that S100A6 may be indispensable for normal proliferation of NIH 3T3 fibroblasts.

SENESCENT FEATURES OF THE S100A6(−) NIH 3T3 FIBROBLASTS

To check if the cell cycle withdrawal of S100A6(−) fibroblasts may be indicative of senescence we examined their β-galactosidase activity, which is the leading hallmark of senescent cells [Dimri et al., 1995]. We found that the amount of dark blue-dyed cells was about 10% in the population of S100A6(−) cells compared to only about 2% with comparable staining intensity among control S100A6(+) cells (Fig. 4A). In most cases intense β-galactosidase staining coincided with polygonal shape and bigger cell area, that is, morphological features typical for senescent cells. Furthermore, as revealed by densitometric analysis of gelatin zymography, the medium collected from the S100A6(−) NIH 3T3 fibroblast cultures was more abundant in gelatinase activity (3.65 ± 0.02, arbitrary units) than that from control fibroblasts (2.18 ± 0.05). Based on the apparent molecular mass, the altered activity could be ascribed to matrix metalloproteinase 2 (MMP2), a recognized marker of senescence [Campisi et al., 1996] while the activity of MMP9 did not change (Fig. 4B). Thus, these observations together with morphological changes and the cell cycle results, suggest that S100A6 deficiency induces senescence-like features in NIH 3T3 fibroblasts.

CHANGES IN THE CYTOSKELETON AND IN THE ADHESIVE AND MIGRATORY PROPERTIES OF S100A6(−) NIH 3T3 FIBROBLASTS

Phalloidin staining showed differences in actin organization in S100A6(−) and S100A6(+) NIH 3T3 fibroblasts. As it can be seen in Figure 5, control cells possessed stress fibers oriented mostly parallel to the long axis of the cell, whereas in the S100A6(−) cells the directionality of actin stress fibers was less regular. It seemed that the cortical actin filaments were more abundant in S100A6(-) cells suggesting formation of lamellipodial or filopodial extensions. Indeed, immunocytochemistry performed with anti-vinculin

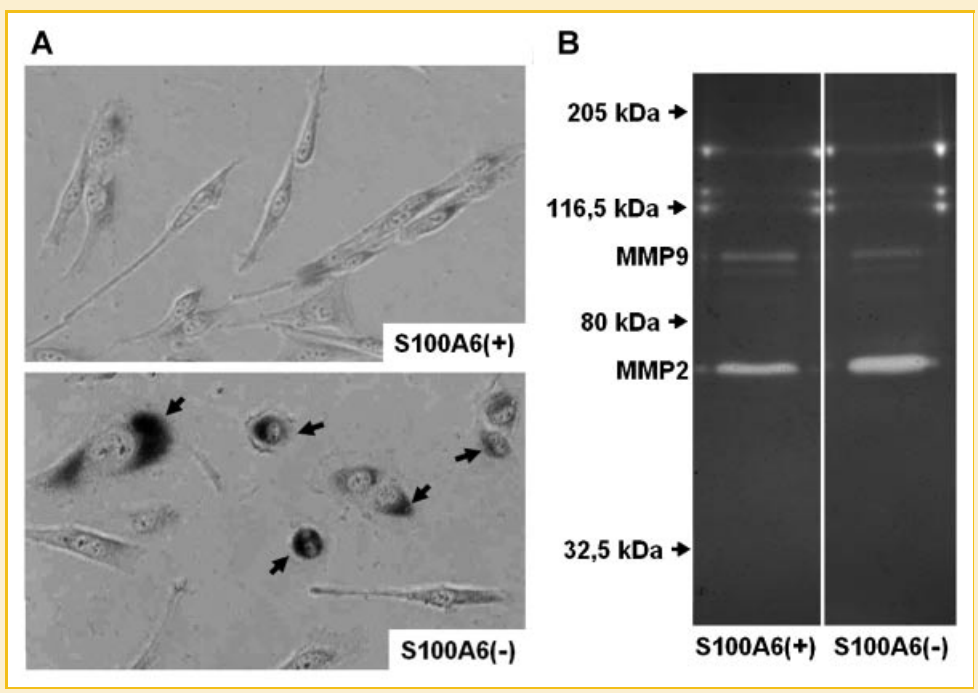

Fig. 4. Markers of cell senescence. A: β-galactosidase staining. The activity of senescence-associated β-galactosidase in S100A6(+) and S100A6(−) NIH 3T3 fibroblasts is visualized by dark blue staining and indicated by arrows (100× magnification, 4× digital zoom). B: SDS-PAGE zymographic analysis of gelatinase activity in culture medium. S100A6(+) and S100A6(−) NIH 3T3 fibroblasts were cultured in 0.5% FBS for 48 h. Cell medium (15 μl) was analyzed by SDS-PAGE zymography with gelatin as substrate. Gelatinase activity was assigned to MMP2 and MMP9 on the basis of the location of the gelatin-free bands relative to the position of MW standards indicated by arrows. The results of representative experiments out of three performed are presented in A and B.

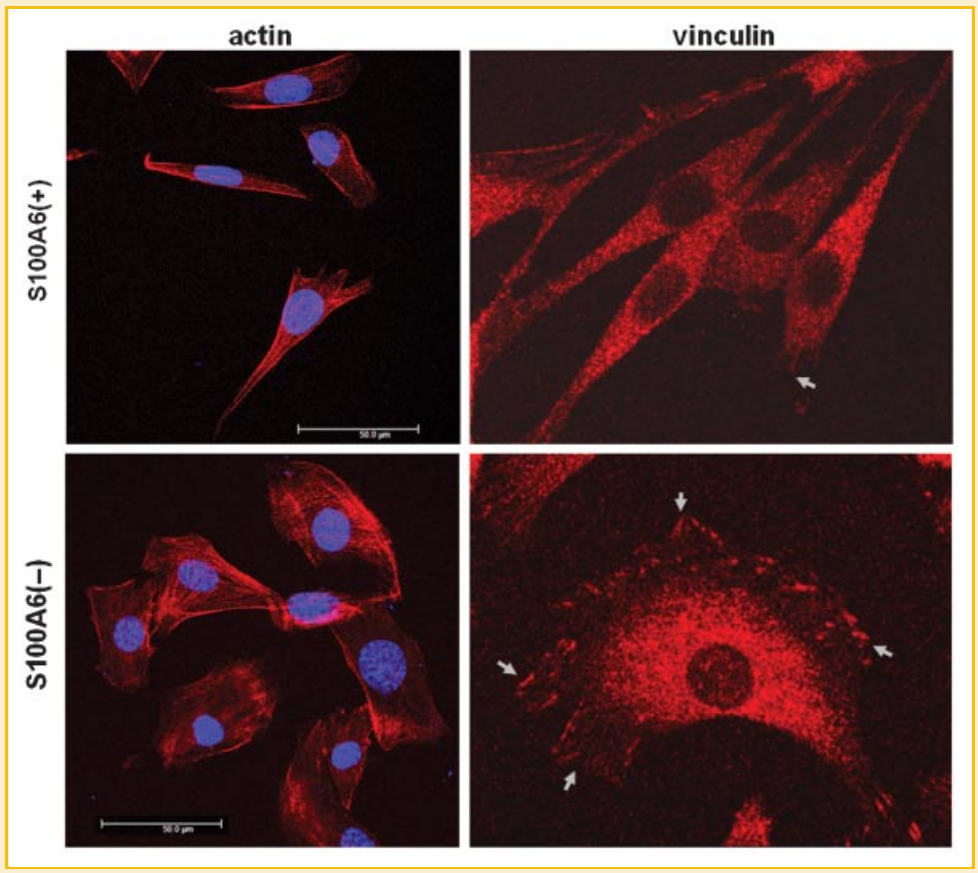

Fig. 5. Actin cytoskeleton and vinculin staining in S100A6(+) and S100A6(−) NIH 3T3 fibroblasts. Cells were plated onto slides, fixed and permeabilized. Actin filaments were stained by phalloidin (left), vinculin was visualized by means of anti-vinculin monoclonal antibody followed by anti-mouse Alexa Fluor 568-conjugated secondary antibody (right). Nuclei were stained with DAPI. Fluorochromes were analyzed by confocal microscopy at 630× magnification; vinculin-stained cells were digitally zoomed (5×). Lamellipodia visualized by vinculin staining are indicated by arrows. [Color figure can be viewed in the online issue, which is available at www.interscience.wiley.com.]

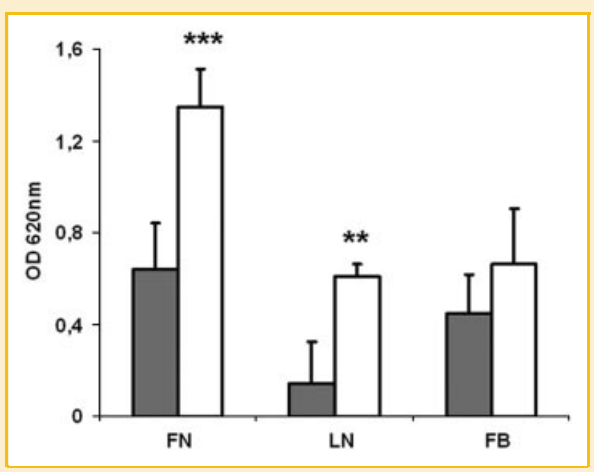

Fig. 6. Colorimetric cell adhesion assay. Stably transfected NIH 3T3 fibroblasts adhered to fibronectin (FN), laminin (LN), and fibrinogen (FB) were quantified colorimetrically at 620 nm after deducting the absorbance derived from wells coated with BSA (negative control). The cells did not adhere to either collagen I or IV. Filled bars represent S100A6(+) and white bars S100A6(−) cells. Statistical analysis was performed using Student's *t*-test. Results from three independent experiments are presented as a mean ± SEM. $^{***}P \leq 0.001$, $^{**}P \leq 0.01$.

antibody revealed that the S100A6(−) cells formed large lamellipodia characterized by abundant punctuate and palisade-like vinculin staining. Interestingly, only few control cells possessed similar lammellipodia. This finding prompted us to examine adhesion of NIH 3T3 fibroblasts with different S100A6 level to surfaces coated with five different extracellular matrix proteins or BSA as a negative control. As could be anticipated on the basis of their morphological features and the fact that they needed longer period of time for successful trypsinization, fibroblasts with diminished S100A6 expression revealed stronger adhesion to laminin, fibronectin and fibrinogen (Fig. 6). Neither cells adhered to collagen I and IV.

In the next step we have compared migratory properties of the S100A6(−) and S100A6(+) NIH 3T3 fibroblasts in an artificial wound (scratch) assay. To keep the focus on cell mobility and minimize the proliferation bias we counted only the cells spotted in the central area of the scratch (corresponding to half of its original width). We found that after 36 h two times more S100A6(−) than S100A6(+) cells in the examined area (Fig. 7A) suggesting that the cytoskeletal rearrangements evoked by S100A6 deficiency resulted in facilitated cell mobility. Differences in cell mobility were also confirmed by random migration analysis. As it can be seen in Figure 7B, S100A6(−) NIH 3T3 fibroblasts changed their position more

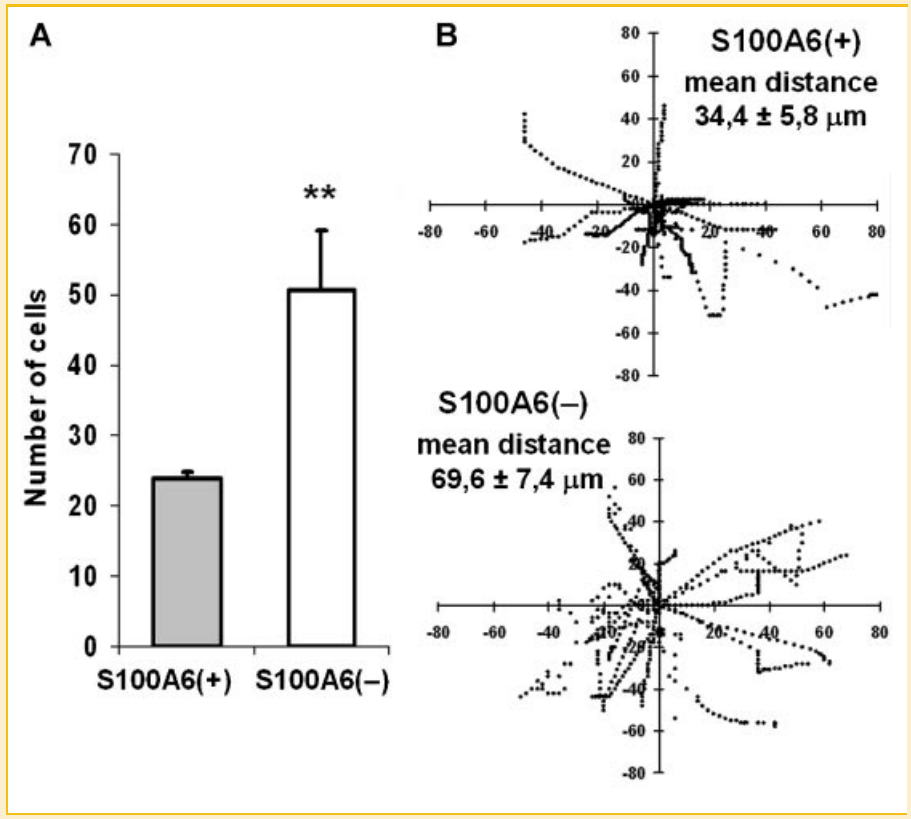

Fig. 7. Measurement of cell migratory properties. A: Scratch assay. A scratch was made with 0.2 ml pipette tip through a confluent culture of S100A6(+) or S100A6(−) NIH 3T3 fibroblasts. The number of cells that migrated into the central area of the scratch was counted after 36 h. Statistical analysis was performed using Student's *t*-test. Results from three independent experiments are presented as a mean ± SEM. $^{**}P \leq 0.01$. B: Random migration analysis. Photographs of 18 stably transfected NIH 3T3 cells seeded on 60 mm dishes coated with 15 μg/ml fibronectin were collected at 100× magnification every 5 min during 2.5 h. Cells were manually traced on each photograph using the ImageJ software. Migration paths were prepared as graphs using the Excel software. The distance scale is in μm. The mean values ± SEM, calculated using Student's *t*-test, are given; $^{***}P \leq 0.001$.

frequently and migrated longer distances (69.6 ± 7.4 μm) than the control cells (34.4 ± 5.8 μm).

DISCUSSION

The effect of changes in cellular S100A6 level evoked either by gene overexpression or knock-down (executed through antisense oligonucleotides or, more recently, siRNA) on various aspects of fibroblast [Breen and Tang, 2003] and other cell physiology [Hwang et al., 2004; Ohuchida et al., 2007] has been studied earlier and supplied data which implicated the S100A6 protein in cell proliferation and cytoskeletal rearrangement. The use of NIH 3T3 fibroblasts stably transfected with siRNA against S100A6 allowed us to study the effects of permanent S100A6 deficiency. Thus, we could not only validate previous observations that cells with decreased S100A6 level proliferate at a slower rate but also establish that many of those cells could not enter the cell cycle in response to serum stimulation and lagged behind the control ones in the G0/G1 phase. The use of two-color flow cytometry allowed us to strictly correlate the apparent retardation in the onset of the cell cycle with low/null cellular S100A6 level. Since the inability to respond to growth factors is a hallmark of cell senescence we looked for senescence markers in the S100A6(−) NIH 3T3 fibroblasts and found that about 10% of these cells were positive for β-galactosidase activity. Furthermore, their cell medium was more enriched in MMP-2 activity, another marker of cell senescence [Campisi et al., 1996], suggesting increased expression/activity of this enzyme in S100A6(−) NIH 3T3 fibroblasts. These cells underwent morphological changes commonly associated with cell senescence and their senescence-like phenotype could also be confirmed by a relative resistance to apoptosis evoked by H_2O_2 (unpublished results). All these observations suggest that the presence of the S100A6 protein may be critical for the fate of a fibroblast, in the sense of cell proliferation versus quiescence/senescence. The supposition that S100A6 may be an important player in these vital processes is corroborated by the original observation that S100A6 mRNA level increased when starved cells were stimulated by serum [Hirschhorn et al., 1984]. Furthermore, it has been found recently that S100A6 knock-down in pancreatic cancer cells led to downregulation of several genes coding for proteins involved in cell proliferation and upregulation of genes known to be negative regulators of gene proliferation [Ohuchida et al., 2007]. Nothing is known however about the exact cell cycle regulatory event for which this protein

may be essential. Our recent studies have shown that S100A6 interacts with p53 [Slomnicki et al., 2009] and studies by other authors mapped this binding to p53 oligomerization domain and showed that it occurred preferably to p53 tetramer [van Dieck et al., 2009]. Although p53 is thought to be indispensable for the onset of cell senescence, whereupon its level might be upregulated [Kulju and Lehman, 1995], a recent study has shown that in senescent human fibroblasts p53 resides predominantly in the cytoplasm in a conformationally altered form [Nishio and Inoue, 2005]. Since we have shown that S100A6 deficiency may impair p53 nuclear translocation [Slomnicki et al., 2009], an intriguing possibility would be that S100A6 contributes to cellular senescence via this mechanism.

Beside the G0/G1 block and cell cycle withdrawal another characteristic feature of the S100A6(−) NIH 3T3 fibroblasts was an increase in cell size accompanied by changes in cell shape and altered motile properties. Immunocytochemical examination revealed altered directionality of actin stress fibers which confirms an earlier observation concerning reorganization of the tropomyosin-associated cytoskeleton filaments [Breen and Tang, 2003]. Since S100A6 interacts with tropomyosin in vitro [Golitsina et al., 1996] changes in the actin filaments may be regarded as a consequence of alterations in the actin–tropomyosin interaction occurring in the absence of S100A6. In a longer time scale such alterations may entail adaptation of the actin cytoskeleton to a newly acquired senescence-like cell shape. Furthermore, vinculin staining revealed that the S100A6(−) NIH 3T3 fibroblasts developed large lamellipodia that contributed to their increased size. In agreement with the appearance of lamellipodia S100A6(−) NIH 3T3 fibroblasts acquired stronger adhesive properties. This is in contrast with results showing that S100A6 downregulation decreased while its overexpression improved adhesion of osteosarcoma cells to collagen I [Luo et al., 2008] and that of Hep3B cells to fibronectin [Cervera et al., 2008]. Discrepancies between those and our results concerning the impact of S100A6 on cell adhesion may be due to different cell types (cancerous and non-cancerous) and extracellular matrix proteins studied or they may reflect the difference between the effects of transient versus long-term, stable S100A6 deficiency on cell adhesion. In this respect, senescent cells reveal stronger adhesive properties than normal cells [Nishio and Inoue, 2005]. We also found that a decrease in S100A6 level resulted in higher cell mobility which was also observed for osteosarcoma cells [Luo et al., 2008]. These improved migratory properties probably result from the totality of changes in fibroblast cytoskeleton organization and cell shape induced by S100A6(−) deficiency.

In conclusion our studies show that the S100A6 protein is indispensable for normal proliferation of mouse NIH 3T3 fibroblasts and that its deficiency evokes senescence-like changes in their morphology and physiology.

ACKNOWLEDGMENTS

Dr. Jolanta Rędowicz is gratefully acknowledged for advice and helpful discussion of matters concerning cell cytoskeleton as well as for donation of the anti-vinculin antibody. Many thanks are due to Jaroslaw Korczynski for help in preparation of the random migration analysis and to Dr. Marta Wisniewska from the International Institute of Molecular and Cell Biology in Warsaw for her expert guidance in performing Real Time PCR experiments. The authors also wish to thank Dr. Anna Filipek for the critical reading of the manuscript. The work was supported by the statutory funds of the Nencki Institute of Experimental Biology.

REFERENCES

Breen EC, Tang K. 2003. Calcyclin (S100A6) regulates pulmonary fibroblast proliferation, morphology, and cytoskeletal organization in vitro. J Cell Biochem 88:848–854.

Campisi J, Dimri G, Hara E. 1996. Control of replicative senescence. In: Johnson TE, Holbrook N, Morrison JH, editors. Handbook of the biology of aging. San Diego: Academic Press. pp 121–149.

Cervera AM, Apostolova N, Crespo FL, Mata M, McCreath KJ. 2008. Cells silenced for SDHB expression display characteristic features of the tumor phenotype. Cancer Res 68:4058–4067.

Courtois-Coutry N, Le Moellic C, Boulkroun S, Fay M, Cluzeaud F, Escoubet B, Farman N, Blot-Chabaud M. 2002. Calcyclin is an early vasopressin-induced gene in the renal collecting duct. Role in the long term regulation of ion transport. J Biol Chem 277:25728–25734.

Dimri GP, Lee X, Basile G, Acosta M, Scott G, Roskelley C, Medrano EE, Linskens M, Rubelj I, Pereira-Smith O, Peacocke M, Campisi J. 1995. A biomarker that identifies senescent human cells in culture and in aging skin in vivo. Proc Natl Acad Sci USA 92:9363–9367.

Filipek A, Kuźnicki J. 1998. Molecular cloning and expression of a mouse brain cDNA encoding a novel protein target of calcyclin. J Neurochem 70: 1793–1798.

Filipek A, Puzianowska M, Cieslak B, Kuznicki J. 1993. Calcyclin–Ca(2+)-binding protein homologous to glial S-100 beta is present in neurons. Neuroreport 4:383–386.

Filipek A, Wojda U, Leśniak W. 1995. Interaction of calcyclin and its cyanogen bromide fragments with annexin II and glyceraldehyde 3-phosphate dehydrogenase. Int J Biochem Cell Biol 27:1123–1131.

Golitsina NL, Kordowska J, Wang CL, Lehrer SS. 1996. Ca^{2+}-dependent binding of calcyclin to muscle tropomyosin. Biochem Biophys Res Commun 220:360–365.

Hirschhorn RR, Aller P, Yuan ZA, Gibson CW, Baserga R. 1984. Cell-cycle-specific cDNAs from mammalian cells temperature sensitive for growth. Proc Natl Acad Sci USA 81:6004–6008.

Hwang R, Lee EJ, Kim MH, Li SZ, Jin YJ, Rhee Y, Kim YM, Lim SK. 2004. Calcyclin, a Ca2+ ion-binding protein, contributes to the anabolic effects of simvastatin on bone. J Biol Chem 279:21239–21247.

Joo JH, Yoon SY, Kim JH, Paik SG, Min SR, Lim JS, Choe IS, Choi I, Kim JW. 2008. S100A6 (calcyclin) enhances the sensitivity to apoptosis via the upregulation of caspase-3 activity in Hep3B cells. J Cell Biochem 103: 1183–1197.

Komatsu K, Andoh A, Ishiguro S, Suzuki N, Hunai H, Kobune-Fujiwara Y, Kameyama M, Miyoshi J, Akedo H, Nakamura H. 2000. Increased expression of S100A6 (Calcyclin), a calcium-binding protein of the S100 family, in human colorectal adenocarcinomas. Clin Cancer Res 6:172–177.

Kossakowska AE, Edwards DR, Prusinkiewicz C, Zhang MC, Guo D, Urbanski SJ, Grogan T, Marquez LA, Janowska-Wieczorek A. 1999. Interleukin-6 regulation of matrix metalloproteinase (MMP-2 and MMP-9) and tissue inhibitor of metalloproteinase (TIMP-1) expression in malignant non-Hodgkin's lymphomas. Blood 94:2080–2089.

Kucharczak J, Pannequin J, Camby I, Decaestecker C, Kiss R, Martinez J. 2001. Gastrin induces over-expression of genes involved in human U373 glioblastoma cell migration. Oncogene 20:7021–7028.

Kulju KS, Lehman JM. 1995. Increased p53 protein associated with aging in human diploid fibroblasts. Exp Cell Res 217:336–345.

Kuznicki J, Kordowska J, Puzianowska M, Wozniewicz BM. 1992. Calcyclin as a marker of human epithelial cells and fibroblasts. Exp Cell Res 200:425–430.

Lesniak W, Szczepanska A, Kuznicki J. 2005. Calcyclin (S100A6) expression is stimulated by agents evoking oxidative stress via the antioxidant response element. Biochim Biophys Acta 1744:29–37.

Lesniak W, Slomnicki LP, Kuznicki J. 2007. Epigenetic control of the S100A6 (calcyclin) gene expression. J Invest Dermatol 127:2307–2314.

Luo X, Sharff KA, Chen J, He TC, Luu HH. 2008. S100A6 expression and function in human osteosarcoma. Clin Orthop Relat Res 466:2060–2070.

Nishio K, Inoue A. 2005. Senescence-associated alterations of cytoskeleton: extraordinary production of vimentin that anchors cytoplasmic p53 in senescent human fibroblasts. Histochem Cell Biol 123:263–273.

Nowotny M, Spiechowicz M, Jastrzębska B, Filipek A, Kitagawa K, Kuźnicki J. 2003. Calcium-regulated interaction of Sgt1 with S100A6 (calcyclin) and other S100 proteins. J Biol Chem 278:26923–26928.

Ohuchida K, Mizumoto K, Yu J, Yamaguchi H, Konomi H, Nagai E, Yamaguchi K, Tsuneyoshi M, Tanaka M. 2007. S100A6 is increased in a stepwise manner during pancreatic carcinogenesis: clinical value of expression analysis in 98 pancreatic juice samples. Cancer Epidemiol Biomarkers Prev 16:649–654.

Santamaria-Kisiel L, Rintala-Dempsey AC, Shaw GS. 2006. Calcium-dependent and -independent interactions of the S100 protein family. Biochem J 396:201–214.

Slomnicki LP, Nawrot B, Lesniak W. 2009. S100A6 binds p53 and affects its activity. Int J Biochem Cell Biol 41:784–790.

van Dieck J, Fernandez-Fernandez MR, Veprintsev DB, Fersht AR. 2009. Modulation of the oligomerization state of p53 by differential binding of proteins of the S100 family to p53 monomers and tetramers. J Biol Chem 284:13804–13811.

Weterman MAJ, Stoopen GM, van Muijen GNP, Kuznicki J, Ruiter DJ, Bloemers HPJ. 1992. Expression of calcyclin in human melanoma cell lines correlates with metastatic behavior in nude mice. Cancer Res 52:1291–1296.

Zeng FY, Gerke V, Gabius HJ. 1993. Identification of annexin II, annexin VI and glyceraldehyde-3-phosphate dehydrogenase as calcyclin-binding proteins in bovine heart. Int J Biochem 25:1019–1027.